**CSIRO** PUBLISHING

# *Australian Journal of Physics*

Volume 50, 1997
© CSIRO Australia 1997

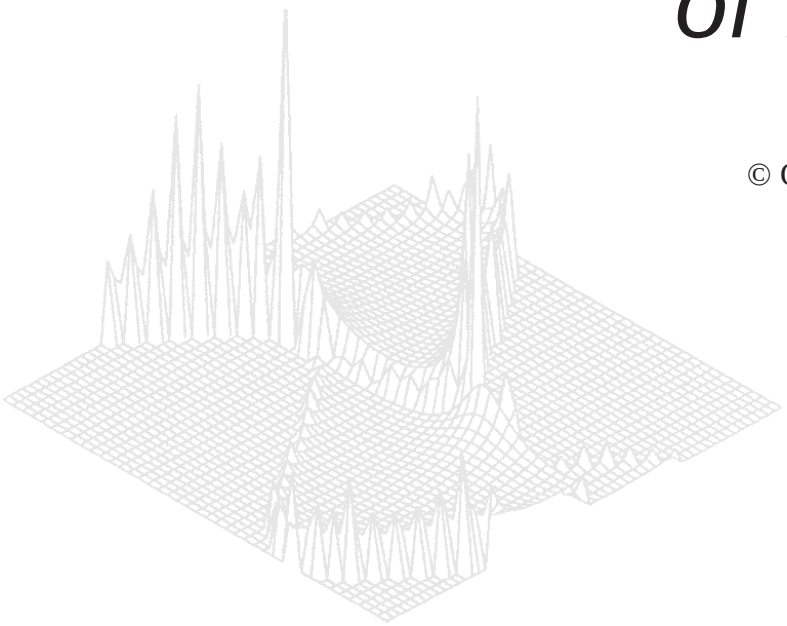

A journal for the publication of
original research in all branches of physics

**www.publish.csiro.au/journals/ajp**

All enquiries and manuscripts should be directed to
*Australian Journal of Physics*
**CSIRO** PUBLISHING
PO Box 1139 (150 Oxford St)
Collingwood Telephone: 61 3 9662 7626
Vic. 3066 Facsimile: 61 3 9662 7611
Australia Email: peter.robertson@publish.csiro.au

Published by **CSIRO** PUBLISHING
for CSIRO Australia and
the Australian Academy of Science

*Aust. J. Phys.*, 1997, **50**, 79–93

# Spin Structure Functions of the Nucleon and Twist-3 Operators in QCD*

*Kazuhiro Tanaka*

Department of Physics, Juntendo University,
Inba-gun, Chiba 270–16, Japan.

email: tanakak@rikaxp.riken.go.jp

*Abstract*

We investigate the twist-3 spin-dependent parton distribution functions $h_L(x, Q^2)$ and $g_T(x, Q^2)$. We discuss the physical relevance of the parton distributions from the view point of the factorization theorem in QCD. A unique feature of the 'measurable' higher-twist distributions $h_L$ and $g_T$ is emphasized. We investigate the $Q^2$-evolution of $h_L$ and $g_T$ in the framework of the renormalization group and standard QCD perturbation theory. We calculate the anomalous dimension matrix for the twist-3 operators for $h_L$ and $g_T$ in the one-loop order. The operator mixing among the relevant twist-3 operators, including the operators proportional to the QCD equations of motion, is treated properly in a consistent scheme. Implications for future experiments are also discussed.

## 1. Introduction

There are various hard processes which are characterized by the large momentum squared $Q^2$: deeply inelastic scattering (DIS), $l+H \to l'+X$ ($H, H'$ denote hadrons, and $l, l'$ denote leptons); the Drell–Yan (DY) processes, $H + H' \to l^+ + l^- + X$; jet production, $H + H' \to \text{jet} + X$; heavy quark production, $H + H' \to \text{heavy quark} + X$, etc.

The basis for the application of perturbative QCD to hard processes is provided by factorization theorem in QCD [1, 2]: Consider the Bjorken limit where $Q^2 \to \infty$ with the Bjorken variable $x$ fixed; $x$ has the physical meaning as the momentum fraction carried by a parton in a hadron. Then the theorem states that the cross section for hard processes is given as the product, or more precisely, the convolution of the two parts: one is the 'hard part', which contains all dependence on the large momentum $Q$; the other is the 'soft part', which depends in an essential way on the QCD scale parameter $\Lambda_{\rm QCD}$. The two parts are divided at the renormalization scale $\mu$; the hard (soft) part involves the momenta larger (smaller) than $\mu$. The hard part corrresponds to the hard scattering cross section

* Refereed paper based on a contribution to the Japan–Australia Workshop on Quarks, Hadrons and Nuclei held at the Institute for Theoretical Physics, University of Adelaide, in November 1995.

10.1071/PH96048 0004-9506/97/010079$05.00

for the partons (quarks and gluons), while the soft part corresponds to parton distribution functions in a hadron. Due to the dependence on the large $Q^2$ and due to asymptotic freedom of QCD, the hard part can be systematically calculated by perturbation theory for each process. The soft part is determined by the nonperturbative dynamics of QCD.

The distribution functions are classified by 'twist'. A distribution of twist-$t$ contributes to the physical cross sections with coefficients which contain $t-2$ or more powers of $1/Q$. It is difficult to extract the higher-twist distributions by experiments because they usually constitute small corrections to the leading twist-2 term. However, the twist-3 distributions $h_L$ and $g_T$ [3] are somewhat immune to this difficulty. Both can be extracted as a leading term by measuring appropriate asymmetries in the processes using a polarized beam: $g_T$ is the distribution function corresponding to the transverse spin structure function $g_2$ [4, 5, 6, 7]. Here $g_2$ contributes as a leading term to the asymmetry of the DIS using the tranversely polarized target. Similarly, $h_L$ reveals itself as a leading contribution to the longitudinal–transverse asymmetry in the polarized DY process.

Recently, the first data of $g_2$ have been reported by the SMC [8] (see also [22]). The extensive study of it will be performed in HERMES. The function $h_L$ will be measured in RHIC. These experiments give the data of the distributions at $\mu^2 = Q^2$, i.e. of $g_T(x,Q^2)$ and $h_L(x,Q^2)$. In view of this it is extremely important to develop a theoretical study of these distribution functions based as much as possible on QCD. Among these efforts, the first step is the perturbative QCD prediction of the $Q^2$-evolution of the distribution functions: Owing to the factorization property of hard processes, the $Q^2$-evolution of the distribution functions can be predicted unambiguously in the framework of the renormalization group and QCD perturbation theory. Its prediction is indispensible to extract physical information from experimental data. Furthermore, comparison of the $Q^2$-evolution itself between theory and experiment will provide a deeper test of QCD beyond the conventional twist-2 level.

In this work we investigate the $Q^2$-evolution of $h_L(x,Q^2)$ and $g_T(x,Q^2)$ in the leading logarithmic approximation. We calculate the anomalous dimension matrix for the twist-3 operators for $h_L$ and $g_T$ in the one-loop order. As for $h_L$, there has been no discussion on $Q^2$-evolution. On the other hand, there are a lot of works for $g_T(g_2)$. For example, in ref. [9], Gribov–Lipatov–Altarelli–Parisi-type evolution equation [10] was derived. However, this was carried out in the axial gauge. Ji and Chou [11] computed the anomalous dimension matrix for the twist-3 operators for $g_T$ in the Feynman gauge. But, their results were not identical to those of ref. [9]. Also, in their work, it is not clear how they treated the 'equation-of-motion (EOM) operators' (see Section 3); improper treatment of the EOM operators might cause uncontrollable difficulty.

It is desirable to establish the theoretical prediction of the $Q^2$-evolution of $g_T$, as well as of $h_L$, based on a fully consistent and covariant scheme. Such a scheme has been recently employed in a study of $g_T$ by Kodaira, Yasui and Uematsu [12]. They computed the anomalous dimension matrix for the lowest $(n=2)$ moment of $g_T$, and demonstrated the consistency and efficiency of the method. We extend the computation to the case of $h_L$ [13] and to the general $n$th moment of $g_T$ [14].

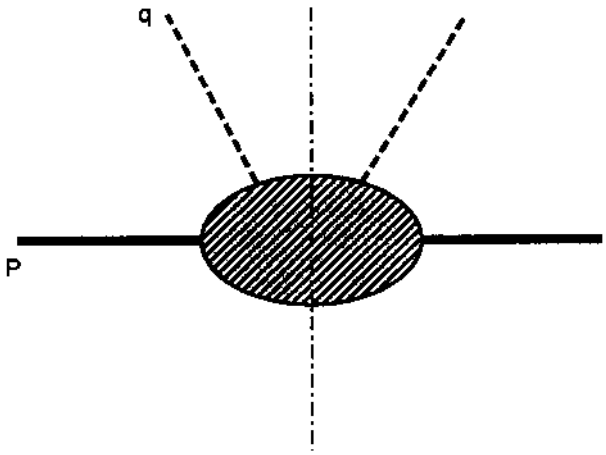


**Fig. 1.** Cut diagram of the forward Compton amplitude between the virtual photon and a hadron, which gives the cross section for the DIS (thick solid lines: hadrons; dashed lines: photons).

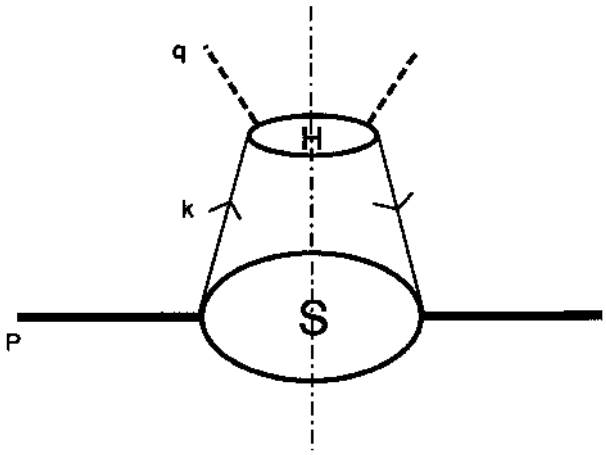


**Fig. 2.** Dominant amplitude in the Bjorken limit for the case of Fig. 1.

## 2. Factorization Theorem and Parton Distribution Functions

Let us examine the factorization theorem in detail by some examples. First, consider the DIS. The cross section for the DIS, $l + H \to l' + X$, is given by the 'cut diagram' of the forward virtual Compton amplitude between the virtual photon with the momentum $q_\mu$ ($q^2 = -Q^2$) and a hadron with the momentum $P_\mu$ ($P^2 = M^2$ with $M$ the hadron mass). In general kinematics, the blob in Fig. 1 contains all the complicated interactions between the virtual photon and a hadron, possibly including the 'soft interactions' where the soft momenta are exchanged. However, drastic simplification occurs if one goes to the Bjorken limit $Q^2 \to \infty$ with $x = Q^2/2P \cdot q$ fixed: The amplitude is dominated by the

contribution which is factorized into the hard and the soft parts (see Fig. 2), and the other complicated contributions are suppressed by the powers of $1/Q$. The factorized amplitude corresponds to the process where a parton carrying the momentum $k = \xi P$ $(0 \leq \xi \leq 1)$ comes out from the soft part, followed by a hard hitting by the virtual photon, and then goes back to the soft part. For example, in the case of the nucleon target, the structure function $F_2$ appears in the DIS cross section, corresponding to the factorized amplitude

$$F_2(x, Q^2) = \sum_a \int_x^1 \frac{d\xi}{\xi} \xi f_{a/H}(\xi, \mu) H_a \left( \frac{x}{\xi}, \frac{Q}{\mu}, \alpha_s(\mu) \right) , \qquad (2 \cdot 1)$$

where $f_{a/H}(\xi, \mu)$ is a parton distribution function corresponding to the soft part and $f_{a/H}$ is interpreted as the probability density to find a parton of type $a$ (= gluon, $u$, $\overline{u}$, $d$, $\overline{d}, \cdots$) in a hadron $H$, carrying a fraction $\xi$ of the hadron's momentum. The summation of eq. $(2 \cdot 1)$ is over all the possible types of parton, $a$. Here $H_a$ denotes the hard scattering cross section between the virtual photon and a parton $a$, corresponding to the hard part. It is calculable systematically by perturbation theory, and the dependence on the strong coupling constant $\alpha_s = g^2/4\pi$ is explicitly shown. The equation $(2 \cdot 1)$ can be proved by analysing directly the Feynman graphs for the forward Compton amplitude in the Bjorken limit [2]. In the present case of the DIS, the equivalent result can be obtained by the operator product expansion [15, 20].

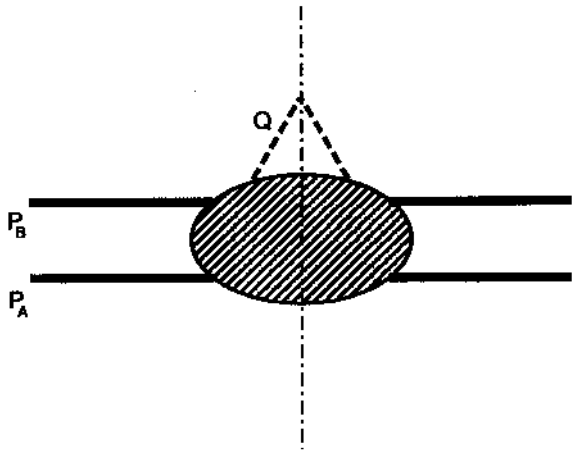


**Fig. 3.** Cut diagram of the forward scattering amplitude between the two hadrons, which gives the cross section for the DY process.

Next we consider the DY processes. The cross section for this process between the hadrons $A$ and $B$, $A + B \to l^+ + l^- + X$, is given by the cut of the forward scattering amplitude between the two hadrons $A$ and $B$ (see Fig. 3). The blob in the figure in general contains all the possible interactions including those with the soft momenta exchanged. In the Bjorken limit $Q^2 \to \infty$ with $x_A x_B = Q^2/s$ fixed $[s = (P_A + P_B)^2$ with $P_{A\mu}$, $P_{B\mu}$ the 4-momenta of the hadrons $A$, $B$; $Q^2$

the invariant mass squared of the final lepton pair], however, the amplitude is dominated by the contribution factorized into the hard and soft parts; the other contributions are suppressed by the powers of $1/Q$. The factorized amplitude corresponds to the process where partons carrying the momenta $k_A = \xi_A P_A$ and $k_B = \xi_B P_B$ come out from the lower and the upper soft parts, followed by hard scattering between them, and then go back to the soft parts (see Fig. 4). Namely, the cross section, accurate up to corrections suppressed by the powers of $1/Q$, is given by

$$\frac{d^2\sigma}{dQ^2 d\Omega} \sim \sum_{a,b} \int_{x_A}^1 d\xi_A \int_{x_B}^1 d\xi_B f_{a/A}(\xi_A, \mu) H_{ab} \left( \frac{x_A}{\xi_A}, \frac{x_B}{\xi_B}, Q, \frac{Q}{\mu}, \alpha_s(\mu) \right) f_{b/B}(\xi_B, \mu) \,. \tag{2·2}$$

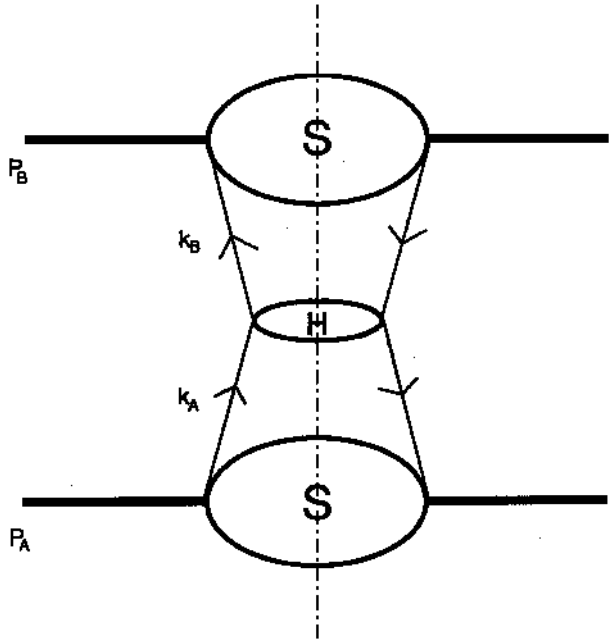


**Fig. 4.** Dominant amplitude in the Bjorken limit for the case of Fig. 3. The photon legs are included in the hard part.

Here $f_{a/A}$ is the parton distribution function for a parton of type $a$ in a hadron $A$, while $H_{ab}$ is the hard scattering cross section between the partons $a$ and $b$, and is calculable by perturbation theory.

We here stress that the soft part appearing in the DY processes has exactly the same structure as the one appearing in the DIS (compare Figs 2 and 4). This demonstrates the universal nature of the soft parts: It is determined completely if one specifies the target. Though it is not calculable by perturbation theory, it can be determined by experiments of some hard processes. For example, if one extracts the soft part for the nucleon target by the DIS experiments, it can be used to describe the DY processes involving the nucleon.

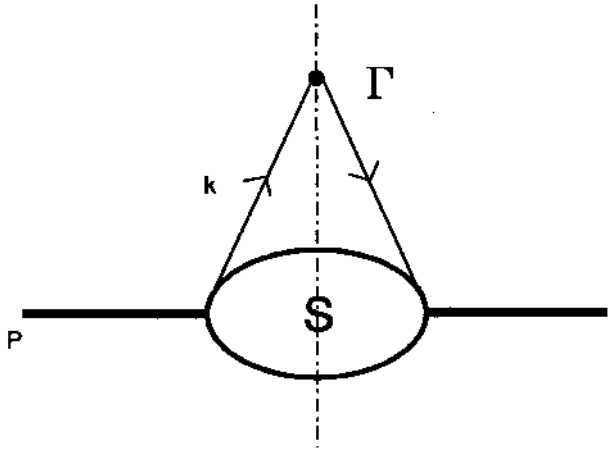


**Fig. 5.** Cut diagram for the soft part (parton distribution function).

Now we recognize that the soft part (parton distribution functions) which universally describes all hard processes is given by the cut diagram of Fig. 5. The corresponding amplitude can be easily written down (we consider the case of the nucleon target here and in the following):

$$\Gamma_{q/N}(x,\mu^2) = \int \frac{d^4k}{(2\pi)^4}\delta(k^+ - xP^+) \int \mathrm{d}^4z\, \mathrm{e}^{ik.z}\langle PS|\overline{\psi}_q(0)\Gamma\psi_q(z)|PS\rangle\,. \qquad (2\cdot3)$$

Here $|PS\rangle$ is the nucleon (mass $M$) state with its momentum $P$ and spin $S$ ($P^2 = M^2, S^2 = -M^2, P\cdot S = 0$), and $\psi$ is the quark field. The bilocal operator is renormalized at the scale $\mu$. We considered the case where the quark of flavour $q$ comes out of the nucleon, followed by the coupling with the vertex $\Gamma$, and then goes back to the nucleon. The quark has $xP^+$ as the plus component of the momentum. (The antiquark or the gluon distribution function is given by a similar formula [2].) To reveal the contents of eq. $(2\cdot3)$, it is convenient to go to the theory quantized on the plane $z^+ = 0$ [$z^\pm = (z^0 \pm z^3)/\sqrt{2}$] in the light-cone gauge $A^+ = 0$ ($A_\mu$ is the gluon field) [2, 3]. We introduce the null vectors $p$ and $n$ by the relations $P_\mu = p_\mu + \frac{M^2}{2}n_\mu, p^2 = n^2 = 0, p\cdot n = 1, n^+ = p^- = 0$, which specify the Lorentz frame of the system. In the light-cone gauge, eq. $(2\cdot3)$ is gauge invariant without the gauge link operator.

There is a degree of freedom to choose the vertex $\Gamma$: $\Gamma$ can be any Dirac matrix depending on which hard process is considered. As shown by Jaffe and Ji [3], one can generate all parton distribution functions (involving the two quark legs) up to twist-4, by substituting all the possible Dirac matrices for $\Gamma$ and by decomposing $\Gamma_{q/N}$ into the independent Lorentz structures: $\Gamma = \gamma^\mu$ gives the twist-2 and the twist-4 distributions $f_1$ and $f_4$ corresponding to the structure functions $F_1, F_2$; $\Gamma = \gamma^\mu\gamma_5$ gives the twist-2, -3, and -4 distributions $g_1, g_T$, and $g_3$ corresponding to the spin structure functions $g_1$, $g_2$; $\Gamma = \sigma^{\mu\nu}$ gives the twist-2, -3, and -4 distributions $h_1, h_L$, and $h_3$; $\Gamma = 1$ gives the twist-3 distribution $e$.

For $\Gamma = \sigma_{\mu\nu} i\gamma_5 = \frac{1}{2}\epsilon_{\mu\nu\lambda\rho}\sigma^{\lambda\rho}$, for example, eq. (2·3) gives

$$\int \frac{d\lambda}{2\pi} e^{i\lambda x} \langle PS|\overline{\psi}(0)\sigma_{\mu\nu} i\gamma_5 \psi(\lambda n)|PS\rangle = 2[h_1(x,\mu^2)(S_{\perp\mu}p_\nu - S_{\perp\nu}p_\mu)/M$$
$$+h_L(x,\mu^2)M(p_\mu n_\nu - p_\nu n_\mu)(S\cdot n) + h_3(x,\mu^2)M(S_{\perp\mu}n_\nu - S_{\perp\nu}n_\mu)]\,, \quad (2\cdot 4)$$

where we have written $S_\mu = S\cdot n p_\mu + S\cdot p n_\mu + S_{\perp\mu}$.

Among these nine distributions, $f_1$, $f_4$ and $e$ are the spin-independent distributions, while the others $(g_1, g_T, g_3, h_1, h_L, h_3)$ are spin-dependent. Because of the chiral property of the vertex $\Gamma$, $f_1, f_4, g_1, g_T$, and $g_3$ are chiral-even while $h_1, h_L, h_3$, and $e$ are chiral-odd [3].

We mention a little more about the chirality and the twist of the distribution functions: If we neglect the small quark mass effects for the light quarks, the chirality is conserved through the propagation of the quark. This means that in the DIS one can measure only the chiral-even distributions because the interaction of the quarks with the gluons as well as with the photons conserves the chirality. On the other hand, in the case of the DY processes the chiral-odd as well as the chiral-even distribution functions can be measured: The quark lines in the r.h.s. of the cut in Fig. 4 can be of the right-handed (left-handed) quark when the quark lines in the l.h.s. are of the left-handed (right-handed) quark.

In the light-cone formalism, the quark fields are decomposed into the 'good' and 'bad' components [16]. Then one can reveal the physical contents of the twist: The twist-2 distributions are literally the 'distributions'; they simply count the number of the quarks having a definite quantum number (flavour, helicity, etc.), and correspond to the parton model. On the other hand, the higher-twist (twist-3 and -4) distributions are the multiparton (quark–gluon) correlation functions which contain the information beyond the parton model [6, 17, 3]: In these cases, one or more gluons are emitted from the soft part and communicate with the hard part, while a quark of momentum fraction $x$ is traveling.

Before ending this section, we emphasize the unique features of $h_L$ and $g_T$: They are the 'measurable' higher-twist distributions, contributing as a leading order term to appropriate asymmetries. They give information on the quark–gluon correlation. Furthermore, $h_L$ corresponds to the chirality-violating processes. Thus, they are expected to provide new information about the hadron structure and the QCD dynamics beyond the conventional structure function data.

## 3. Twist-3 Operators for $h_L$ and $g_T$

In general, twist-3 distributions contain the twist-2 part (analogue of the 'Wilczek–Wandzura piece' of $g_2$[19]) as well as the genuine twist-3 part. For the case of $h_L$:

$$h_L(x,\mu^2) = 2x\int_x^1 dy \frac{h_1(y,\mu^2)}{y^2} + \tilde{h}_L(x,\mu^2) \qquad (x>0)\,, \quad (3\cdot 1)$$

where $h_1$ is a chiral-odd distribution function of twist-2 ('transversity distribution') [18, 3], while $\tilde{h}_L$ is of twist-3. As is well known, the moments of the distribution

functions $\mathcal{M}_n\left[\tilde{h}_L(\mu^2)\right] \equiv \int dx x^n \tilde{h}_L(x,\mu^2)$ are related to the matrix elements of the local composite operators (for the detail, see ref. [3]). Taylor expanding the bilocal operator in the l.h.s. of eq. (2·4), we obtain $\mathcal{M}_n\left[\tilde{h}_L(\mu^2)\right] \sim \langle PS|T_n^{\mu_1\cdots\mu_n}(\mu)|PS\rangle$ with

$$T_n^{\mu_1\cdots\mu_n} = \sum_{l=2}^{[(n+1/2)]} \left(1-\frac{2l}{n+2}\right) R_{nl}^{\mu_1\cdots\mu_n} - \frac{n}{n+2} N_n^{\mu_1\cdots\mu_n} - \frac{n}{n+2} E_n^{\mu_1\cdots\mu_n}\,, \quad (3\cdot2)$$

where $R_{nl}, N_n$, and $E_n$ are the twist-3 operators. Here $R_{nl}$ is defined as

$$R_{nl}^{\mu_1\cdots\mu_n} = \theta_{n-l+2}^{\mu_1\cdots\mu_n} - \theta_l^{\mu_1\cdots\mu_n} \qquad \left(l=2,...,\left[\frac{n+1}{2}\right]\right), \quad (3\cdot3)$$

$$\theta_l^{\mu_1\cdots\mu_n} = \tfrac{1}{2}\mathcal{S}_n \bar{\psi}\sigma^{\alpha\mu_1} i\gamma_5 iD^{\mu_2}\cdots igG^{\mu_l}{}_{\alpha}\cdots iD^{\mu_n}\psi - \text{traces}\,, \quad (3\cdot4)$$

where the covariant derivative $D_\mu = \partial_\mu - igA_\mu$ restores explicit gauge invariance, and $G_{\mu\nu}$ is the gluon field strength tensor. The symbol $\mathcal{S}_n$ symmetrizes the indices $\mu_1,\cdots,\mu_n$. The $N_n$ and $E_n$ are given by

$$N_n^{\mu_1\cdots\mu_n} = \mathcal{S}_n m_q \bar{\psi}\gamma_5\gamma^{\mu_1} iD^{\mu_2}\cdots iD^{\mu_n}\psi - \text{traces} \quad (3\cdot5)$$

with $m_q$ the quark mass, and

$$E_n^{\mu_1\cdots\mu_n} = \tfrac{1}{2}\mathcal{S}_n[\bar{\psi}(i\not{D}-m_q)\gamma_5\gamma^{\mu_1} iD^{\mu_2}\cdots iD^{\mu_n}\psi + \bar{\psi}\gamma_5\gamma^{\mu_1} iD^{\mu_2} \cdots iD^{\mu_n}(i\not{D}-m_q)\psi] - \text{traces}\,. \quad (3\cdot6)$$

The operator $R_{nl}$ explicitly involves the gluon field strength tensor; this implies that the twist-3 distribution $h_L$ in fact represents the effect of quark–gluon correlations. The operator $N_n$ is due to the quark mass effect.

The operator $E_n$ vanishes by the naive use of the QCD equation of motion $(i\not{D}-m_q)\psi = 0$. We call it the 'equation-of-motion (EOM) operator' from now on. We can set it to zero when we take its matrix element with respect to a physical state (such as the nucleon state) [1, 20]. However, this is not an operator identity and the renormalization mixing between $E_n$ and the other twist-3 operators should be taken into account to compute the anomalous dimensions.

Summarizing, for the $n$th moment of $h_L$, $[(n+3)/2]$ gauge-invariant twist-3 operators (3·3)–(3·6) participate. They mix with each other under renormalization (see Section 4).

Next, we discuss the twist-3 operators for $g_T$ [6, 7]. $g_T$ contains the contribution due to the twist-2 distribution $g_1$ as well as the genuine twist-3 part $\tilde{g}_T$:

$$g_T(x,\mu^2) = -g_1(x,\mu^2) + \int_x^1 \frac{dy}{y} g_1(y,\mu^2) + \tilde{g}_T(x,\mu^2)\,. \quad (3\cdot7)$$

Taking the moment of $\tilde{g}_T$, we obtain $\mathcal{M}_n\left[\tilde{g}_T(\mu^2)\right] \sim \langle PS|T_n^{\mu_1\cdots\mu_n\sigma}(\mu)|PS\rangle$ with

$$T_n^{\mu_1\cdots\mu_n\sigma} = \sum_{l=1}^{n-1} \frac{n-k}{n} R_{nl}^{\mu_1\cdots\mu_n\sigma} + N_n^{\mu_1\cdots\mu_n\sigma} + E_n^{\mu_1\cdots\mu_n\sigma}\,. \tag{3·8}$$

The twist-3 operators $R_{nl}, N_n$ and $E_n$ are given by (we consider the case of even $n$ which is relevant for the DIS)

$$R_{nl}^{\mu_1\cdots\mu_n\sigma} = -V_l^{\mu_1\cdots\mu_n\sigma} + V_{n-l}^{\mu_1\cdots\mu_n\sigma} + U_l^{\mu_1\cdots\mu_n\sigma} + U_{n-l}^{\mu_1\cdots\mu_n\sigma} (l = 1, ..., n-1)\,, \tag{3·9}$$

$$V_l^{\mu_1\cdots\mu_n\sigma} = \tfrac{1}{4}\mathcal{S}_n \bar{\psi} i D^{\mu_1}\cdots igG^{\sigma\mu_l}\cdots iD^{\mu_{n-1}} i\gamma^{\mu_n} i\gamma_5\psi - \text{traces}\,, \tag{3·10}$$

$$U_l^{\mu_1\cdots\mu_n\sigma} = -\tfrac{1}{4}\mathcal{S}_n \bar{\psi} i D^{\mu_1}\cdots ig\tilde{G}^{\sigma\mu_l}\cdots iD^{\mu_{n-1}} i\gamma^{\mu_n}\psi - \text{traces}\,, \tag{3·11}$$

$$N_n^{\mu_1\cdots\mu_n\sigma} = \frac{i}{4}\mathcal{S}_n m_q \bar{\psi}[\gamma^\sigma, \gamma^{\mu_1}] i\gamma_5 iD^{\mu_2}\cdots iD^{\mu_n}\psi - \text{traces}\,, \tag{3·12}$$

where $\tilde{G}_{\mu\nu} = \frac{1}{2}\epsilon_{\mu\nu\rho\lambda}G^{\rho\lambda}$, and

$$\begin{aligned} E_n^{\mu_1\cdots\mu_n\sigma} = \frac{i}{8}\mathcal{S}_n \big[&\bar{\psi}(i\not{D} - m_q)\left[\gamma^\sigma, \gamma^{\mu_1}\right] i\gamma_5 iD^{\mu_2}\cdots iD^{\mu_n}\psi \\ &+ \bar{\psi}\left[\gamma^\sigma, \gamma^{\mu_1}\right] i\gamma_5 iD^{\mu_2}\cdots iD^{\mu_n}(i\not{D} - m_q)\psi\big] - \text{traces}\,. \end{aligned} \tag{3·13}$$

These operators are of similar nature with the corresponding operators $R_{nl}, N_n, E_n$ for $h_L$. If we consider the $Q^2$-evolution of the flavour nonsinglet part, there appears no pure gluonic operator for $g_T$. Thus, in this case, the $n+1$ gauge-invariant operators (3·9)–(3·13) participate and mix with each other under renormalization (see Section 4). (For $h_L$, there is no pure gluonic operator even for the flavour singlet case, because of the chiral-odd property.)

## 4. Anomalous Dimension Matrix for Twist-3 Operators

The $Q^2$-evolution of $h_L$ and $g_T$ is determined by the scale dependence of the composite operators discussed in the last section. The scale dependence is governed by the anomalous dimensions of the operators, which appear in the renormalization group equation for the operators [15, 20]. To obtain the anomalous dimensions, we perform the renormalization of the operators. We consider the three-point function with the insertion of the twist-3 operator $O_i$ ($O_i$ symbolically refer to $R_{nl}, E_n$, and $N_n$): $\langle 0|\mathrm{T}O_i(0)\psi(x)\overline{\psi}(y)A_\mu^a(z)|0\rangle$. We compute the one-loop correction to the three-point function in the Feynman gauge (see Fig. 6). We employ the minimal subtraction scheme in the dimensional

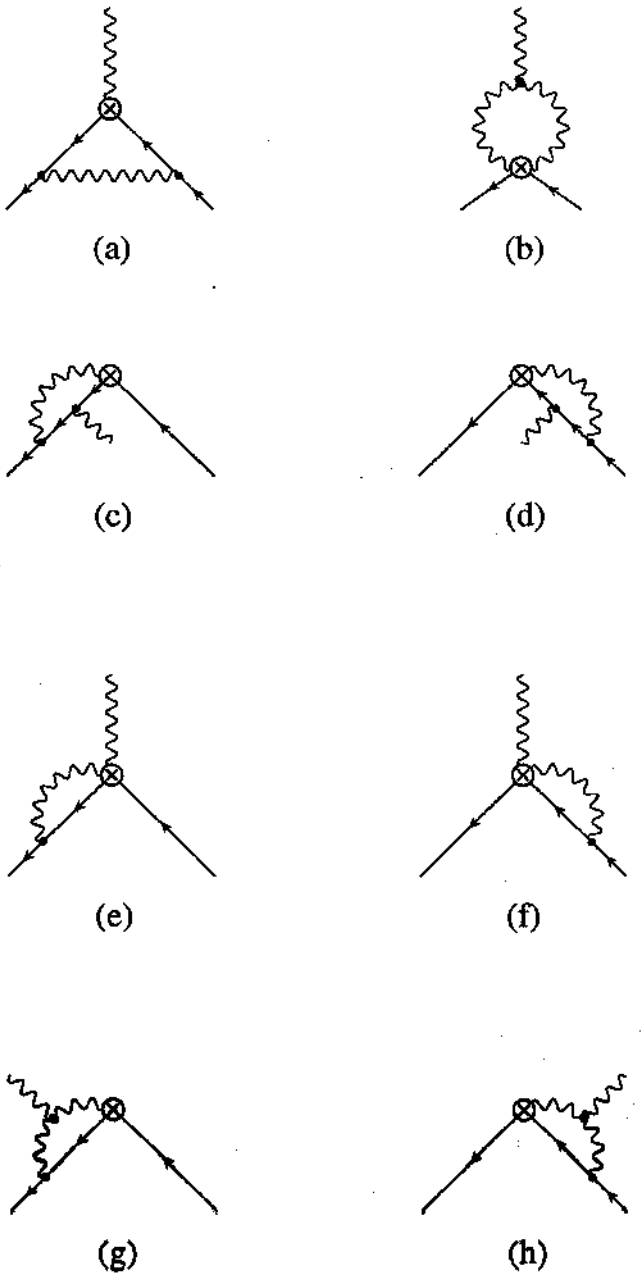


**Fig. 6.** One-particle-irreducible diagrams for the one-loop correction to the three-point function (solid lines: quarks; wavy lines: gluons).

regularization. One important point is that one should keep the external legs of the three-point function off-shell [12]. In this case, the three-point function with $O_i = E_n$ inserted does not vanish, and we can properly treat the renormalization mixing of the EOM operators with the other twist-3 operators.

We summarize here the final result in the following matrix form for $h_L$ (for details of the computation see ref. [13]):

$$\begin{pmatrix} R^B_{nl} \\ E^B_n \\ N^B_n \end{pmatrix} = \begin{pmatrix} Z_{lm}(\mu) & Z_{lE}(\mu) & Z_{lN}(\mu) \\ 0 & Z_{EE}(\mu) & 0 \\ 0 & 0 & Z_{NN}(\mu) \end{pmatrix} \begin{pmatrix} R_{nm}(\mu) \\ E_n(\mu) \\ N_n(\mu) \end{pmatrix}$$

$$\left( l, m = 2, \cdots, \left[ \frac{n+1}{2} \right] \right). \quad (4\cdot 1)$$

The operators in the l.h.s with superscript '$B$' are the bare operators, while those in the r.h.s. are the renormalized ones. If we express the renormalization constant $Z_{ij}$ as

$$Z_{ij} = \delta_{ij} + \frac{g^2}{8\pi^2(4-D)} X_{ij} \qquad \left( i, j = 2, \cdots, \left[ \frac{n+1}{2} \right], E, N \right), \qquad (4\cdot 2)$$

with $D$ the space–time dimension, the anomalous dimension matrix for the twist-3 operators $R_{nl}$, $E_n$ and $N_n$ take the form of the upper triangular matrix as

$$\gamma_{ij} = -\frac{g^2}{8\pi^2} X_{ij} \,. \qquad (4\cdot 3)$$

The analytic expression for $X_{ij}$ is rather complicated; we refer the readers to ref. [13]. In the next section we will show some examples of the $Q^2$-evolution obtained by using the results.

The results for $g_T$ can be summarized similarly to eqs (4·1)–(4·3) but with $l, m = 1,\ ...,\ n-1$ [14]. We present the relevant components of $X_{ij}$ $(i, j = 1, \cdots n-1, E, N)$:

$$X_{lm} = (2C_F - C_G) \left[ \frac{(-1)^{l+m}(n+l-m)\ {}_{n-1}C_{m-1}}{n(l-m)\ {}_{n-1}C_{l-1}} + \frac{2(-1)^m\ {}_lC_m}{l(l+1)(l+2)} \right]$$

$$+ C_G \frac{(m+1)(m+2)}{(l+1)(l+2)(l-m)} \qquad (1 \le m \le l-1)\,, \qquad (4\cdot 4)$$

$$X_{ll} = (2C_F - C_G)\left[\frac{1}{n} + \frac{2(-1)^l}{l(l+1)(l+2)} - \frac{(-1)^l}{n-l+1}\right] + C_F\,(3 - 2S_l - 2S_{n-l})$$

$$+ C_G\left(-S_l - S_{n-l} + \frac{1}{l} - \frac{1}{l+1} - \frac{1}{l+2} - \frac{1}{n-l+1}\right), \qquad (4\cdot5)$$

$$X_{lm} = (2C_F - C_G)\left[\frac{(-1)^{l+m}(n-l+m)\ {}_{n-1}C_m}{n(m-l)\ {}_{n-1}C_l} - \frac{(-1)^{n-m}\ {}_{n-l-1}C_{n-m-1}}{n-l+1}\right]$$

$$+ C_G\frac{(n-m)(n-m+1)}{(n-l)(n-l+1)(m-l)} \qquad (l+1 \le m \le n-1)\,, \quad (4\cdot6)$$

$$X_{lE} = -2C_F\frac{1}{(l+1)(l+2)}\,, \qquad (4\cdot7)$$

where $S_n = \sum_{j=1}^{n} 1/j$ and $C_F = (N_c^2-1)/2N_c$, $C_G = N_c$ are the Casimir operators of the colour gauge group SU($N_c$), and ${}_nC_l$ denotes the binomial coefficient. The result shows that the EOM operator does in fact mix with the other operators. We here note that our results are not identical to those of ref. [11], but agree with those of ref. [9].

## 5. Examples of $Q^2$-evolution

We present some examples of the $Q^2$-evolution of the twist-3 distributions $\tilde{h}_L(x,Q^2)$ and $\tilde{g}_T(x,Q^2)$ based on the results of the previous sections. For simplicity, we shall consider a distribution for one flavour of massless quark. In this case the operator $N_n$ does not contribute.

For the third and fourth moments of $\tilde{h}_L$, and for the second moment of $\tilde{g}_T$, only one twist-3 operator $R_{nl}$ contributes. For $\tilde{h}_L$, for example, we obtain the $Q^2$-evolution:

$$\mathcal{M}_3[\tilde{h}_L(Q^2)] = \tfrac{1}{5}b_{3,2}(\mu)\left(\frac{\alpha_s(Q^2)}{\alpha_s(\mu^2)}\right)^{1\cdot284};$$

$$\mathcal{M}_4[\tilde{h}_L(Q^2)] = \tfrac{1}{3}b_{4,2}(\mu)\left(\frac{\alpha_s(Q^2)}{\alpha_s(\mu^2)}\right)^{1\cdot357}, \qquad (5\cdot1)$$

where we set [see eq. $(3\cdot2)$ and note $\langle PS|E_n|P'S'\rangle = 0$]:

$$\langle PS|R_{nl}^{\mu_1\cdots\mu_n}(\mu^2)|PS\rangle = 2b_{n,l}(\mu^2)M\mathcal{S}_n(S^{\mu_1}P^{\mu_2}\cdots P^{\mu_n} - \text{traces})\,. \qquad (5\cdot2)$$

These curves normalized at $\mu = 1$ GeV are shown in Fig. 7. Here and below we set $N_f = 3$ and $\Lambda_{\rm QCD} = 0\cdot5$ GeV. For comparison, we also plotted the moments of the twist-2 distributions $f_1$ [15] and $h_1$ [21, 13]. From this figure, one can

clearly see that the third moment of the twist-3 distribution evolves significantly faster than that of the twist-2 one.

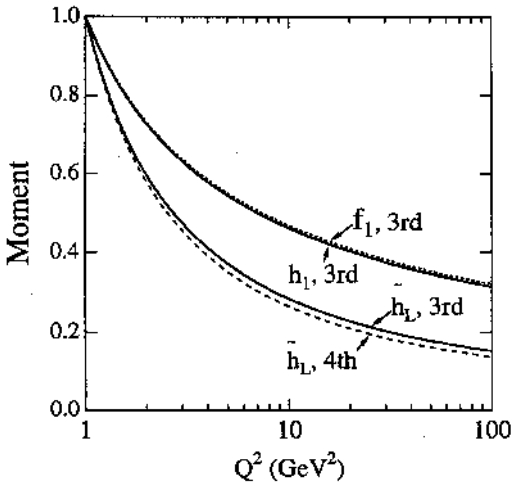


**Fig. 7.** The $Q^2$-evolution of the third and fourth moments of $\tilde{h}_L(x, Q^2)$ normalized at $\mu = 1$ GeV. The third moments of twist-2 distributions $f_1$ and $h_1$ are also plotted for comparison.

For $n = 5$, the anomalous dimension for $\tilde{h}_L$ becomes the $2 \times 2$ matrix, and we get

$$\mathcal{M}_5[\tilde{h}_L(Q^2)] = (0{\cdot}416 b_{5,2}(\mu) + 0{\cdot}193 b_{5,3}(\mu)) \left(\frac{\alpha_s(Q^2)}{\alpha_s(\mu^2)}\right)^{1{\cdot}435} + (0{\cdot}013 b_{5,2}(\mu) - 0{\cdot}050 b_{5,3}(\mu)) \left(\frac{\alpha_s(Q^2)}{\alpha_s(\mu^2)}\right)^{2{\cdot}005} . \quad (5{\cdot}3)$$

In principle, if one measures $\mathcal{M}_5[\tilde{h}_L(Q^2)]$ at two different values of $Q^2$ with sufficient accuracy, one could fix the two matrix elements $b_{5,2}(\mu)$ and $b_{5,3}(\mu)$, and the measurement of $\mathcal{M}_5[\tilde{h}_L(Q^2)]$ at different $Q^2$ provides a test of the QCD evolution. Since we do not have any physical insight into these matrix elements, we plotted $\mathcal{M}_5[\tilde{h}_L(Q^2)]$ normalized at $\mu = 1$ GeV in Fig. 8 with the four moderate values of $\lambda(\mu) = b_{5,3}(\mu)/b_{5,2}(\mu) = -4{\cdot}0, -2{\cdot}0, 1{\cdot}0$ and $4{\cdot}0$ at $\mu = 1$ GeV. We see that the results strongly depend on the value of $\lambda(\mu)$. This fact suggests that a nonperturbative technique of QCD can be tested by comparison of their prediction on $\lambda(\mu)$ with future experiments.

As a measure of the asymptotic behaviour of the $Q^2$-evolution, we have plotted in Fig. 9 the lowest eigenvalues of the matrix $\tilde{\gamma}_{lm} \equiv -X_{lm}/(11 - \frac{2}{3}N_f)$ for $\tilde{h}_L$ and $\tilde{g}_T$ as a function of $n$ ($l, m = 2, .., [\frac{n+1}{2}]$ for $\tilde{h}_L$ and $1, .., n-1$ for $\tilde{g}_T$). For comparison, the results for $h_1$ and $f_1$ are also shown. The larger lowest-eigenvalue corresponds to the stronger $Q^2$-dependence for large $Q^2$. From this figure we expect that the moment of the twist-3 distributions evolves faster than that of

the twist-2 distributions. If one looks in more detail at Fig. 9 one sees that the chiral-odd distribution functions, $h_1$ and $\tilde{h}_L$, evolve slightly faster than the chiral-even ones with the same twist, $f_1$, $g_1$ and $\tilde{g}_T$.

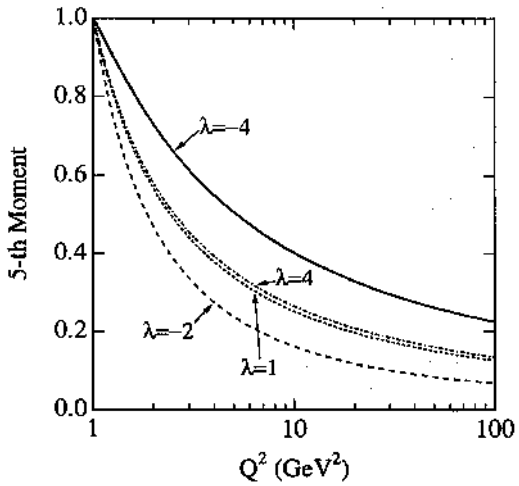


**Fig. 8.** The $Q^2$-evolution of the fifth moment of $\tilde{h}_L(x, Q^2)$ normalized at $\mu = 1$ GeV for the four moderate values of $\lambda(\mu) = -4{\cdot}0, -2{\cdot}0, 1{\cdot}0$ and $4{\cdot}0$.

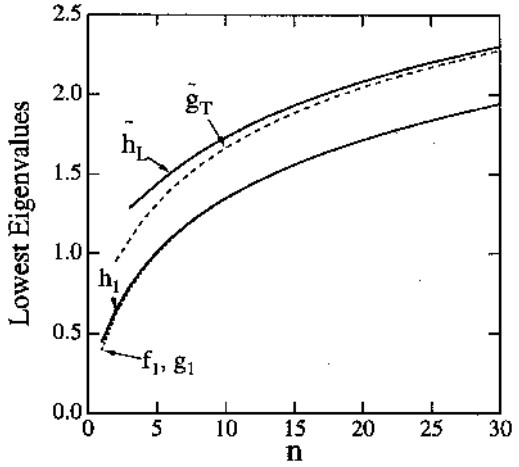


**Fig. 9.** Smallest eigenvalues of $\tilde{\gamma}$ as a function of the dimension of the moment, $n$.

## 6. Summary

In this paper we discussed the 'measurable' twist-3 distribution functions $h_L$ and $g_T$. Both will be measured in future collider experiments.

We made a prediction of the $Q^2$-evolution of $h_L(x, Q^2)$ and $g_T(x, Q^2)$ based on the renormalization group and QCD perturbation theory. We employed a fully consistent and covariant scheme. We computed the anomalous dimension matrix

for the twist-3 operators for $h_L$ and $g_T$ by evaluating the off-shell three-point function. There appear novel features in the renormalization of the twist-3 operators: Participation of the increasing number ($\sim n$) of independent operators for the moments of increasing $n$; renormalization mixing of the EOM operators.

As for the $Q^2$-evolution, we found the following general pattern: The twist-3 distributions evolve faster than the twist-2 ones; the chiral-odd distributions evolve faster than the chiral-even ones; the $Q^2$-evolution of the higher moments depends strongly on the value of the nucleon matrix elements of the twist-3 operators $\langle PS|R_{nl}(\mu)|PS\rangle$.

We hope that these peculiar features of the twist-3 distributions will be revealed in future measurements of $h_L$ and $g_T$.

**Acknowledgment**

The author would like to thank Yuji Koike, Jiro Kodaira, Yoshiaki Yasui and Tsuneo Uematsu for collaboration on the subject discussed in this paper.

**Note added in proof**

Recently it has been proved [23] that the twist-3 chiral-odd parton distributions $h_L(x, q^2)$ and $e(x, Q^2)$ obey simple GLAP evolution equations in the limit $N_c \to \infty$ : In this limit the operators involving the gluon field strength tensor effectively decouple from the evolution equation. Combined with a similar result for $g_T(x, Q^2)$ [24], this demonstrates that simplification for $N_c \to \infty$ is a universal phenomenon for all twist-3 nonsinglet parton distributions. For phenomenology, these results provide a powerful framework for comparision with experimental data, since the results are valid to an accuracy of $O(1/N_c^2)$ which is numerically very small.

**References**

[1] H. D. Politzer, Nucl. Phys. **B172** (1980) 349.
[2] For a general review of QCD factorization see, for example, J. C. Collins, D. Soper and G. Sterman, 'Factorization of hard processes in QCD', *In* 'Perturbative Quantum Chromodynamics' (Ed. A. H. Mueller) (World Scientific, Singapore, 1989).
[3] R. L. Jaffe and X. Ji, Phys. Rev. Lett. **67** (1991) 552; Nucl. Phys. **B375** (1992) 527.
[4] M. A. Ahmed and G. G. Ross, Nucl. Phys. **B111** (1976) 441.
[5] J. Kodaira, S. Matsuda, T. Muta, K. Sasaki and T. Uematsu, Phys. Rev. **D20** (1979) 627; J. Kodaira, S. Matsuda, K. Sasaki and T. Uematsu, Nucl. Phys. **B159** (1979) 99.
[6] E. V. Shuryak and A. I. Vainshtein, Nucl. Phys. **B201** (1982) 141.
[7] R. L. Jaffe, Comments Nucl. Part. Phys. **19** (1990) 239.
[8] D. Adams *et al.*, Phys. Lett. **B336** (1994) 125.
[9] A. P. Bukhvostov, E. A. Kuraev and L. N. Lipatov, Sov. Phys. JETP **60** (1984) 22.
[10] V. N. Gribov and L. N. Lipatov, Sov. J. Nucl. Phys. **15** (1972) 438; L. N. Lipatov, Sov. J. Nucl. Phys. **20** (1975) 94; G. Altarelli and G. Parisi, Nucl. Phys. **B126** (1977) 298.
[11] X. Ji and C. Chou, Phys. Rev. **D42** (1990) 3637.
[12] J. Kodaira, Y. Yasui and T. Uematsu, Phys. Lett. **B344** (1995) 348; Y. Yasui, Prog. Theor. Phys. Suppl. **120** (1995) 239.
[13] Y. Koike and K. Tanaka, Phys. Rev. **D51** (1995) 6125; Prog. Theor. Phys. Suppl. **120** (1995) 247.
[14] J. Kodaira, Y. Yasui, K. Tanaka and T. Uematsu, hep-ph/9603377, Phys. Lett. **B**, in press.

[15] T. Muta, 'Foundations of Quantum Chromodynamics' (World Scientific, Singapore, 1987).
[16] J. B. Kogut and D. E. Soper, Phys. Rev. **D1** (1970) 2901.
[17] R. L. Jaffe and M. Soldate, Phys. Lett. **B105** (1981) 467; Phys. Rev. **D26** (1982) 49.
[18] J. Ralston and D. E. Soper, Nucl. Phys. **B152** (1979) 109.
[19] W. Wandzura and F. Wilczek, Phys. Lett. **B172** (1975) 195.
[20] J. C. Collins, 'Renormalization' (Cambridge Univ. Press, 1984).
[21] X. Artru and M. Mekhfi, Z. Phys. **C45** (1990) 669.
[22] K. Abe *et al.*, Phys. Rev. Lett. **76** (1996) 587.
[23] I. I. Balitsky, V. M. Bruan, Y. Koike and K. Tanaka, hep-ph/6605439, Phys. Rev. Lett. **77** (1996) in press.
[24] A. Ali, V. M. Braun and G. Hiller, Phys. Lett. **B266** (1991) 117.